UNIVERSITY OF CALIFORNIA SAN DIEGO

Mechanism of Neurotransmitter-Receptor Matching in Embryonic Skeletal Muscle *in vivo*

A Thesis submitted in partial satisfaction of the
requirements for the degree Master of Science

in

Biology

by

Yunxin Wang

Committee in Charge:

Professor Nicholas Spitzer, Chair
Professor Yishi Jin
Professor Byungkook Lim

2018

The Thesis of Yunxin Wang is approved, and it is acceptable in quality and form for publication on microfilm and electronically:

_____

_____

_____

Chair

University of California San Diego

2018

DEDICATION

This Thesis is dedicated to my family for their unconditional love and support. I appreciate your sacrifices and I wouldn't have been able to get to this stage without you all.

This is also dedicated to all my friends who have walked alongside me during the last three years.

Thank you all so much.

TABLE OF CONTENTS

LIST OF FIGURES

ACKNOWLEDGEMENTS

The last two and a half years would not have been possible without such a great group of people who have helped in advancing my scientific education. I would like to express my deep appreciation and gratitude to Dr. Nick Spitzer for the patient guidance and mentorship he provided to me, all the way from when I took cellular neurobiology, through to completion of this degree. Dr. Spitzer has always been a lifesaver through all the hardships and troubles I have faced. Thank you for allowing me to be a part of the Spitzer lab family and for your support as my committee chair and principal investigator. I am truly fortunate to have had the opportunity to work with you.

I would also like to thank my committee members, Dr. Yishi Jin and Dr. Byungkook Lim, for their time and support. They have been extremely accommodating despite their busy schedules. Thank you for volunteering to be a part of my thesis committee.

Next, I would like to acknowledge my mentor and teacher, Dr. Dena Weinberger, for guiding me through the project. Dr. Weinberger has taught me experimental design, lab techniques, and data analysis, and I could not imagine having a better teacher. Thank you for turning me into an independent, critical-thinking scientist.

Finally, I would like to recognize all the past and present members of the Spitzer lab and the Berg lab for the contributions that each of them made to my intellectual growth during my years at Pacific Hall. I would like to thank Alex Glavis-Bloom for technical support and animal care, and for his insight and help with my project. I would like to thank Alex, Hui-quan Li, Stefania Zambetti, Swetha Godavarthi, Vince Luczak, Marta Pratelli, Da Meng, Nandu Prakash, and Davide Dulcis for thought-provoking suggestions and rigorous discussions. You have all been like a family to me and I will never forget all the memories we shared together.

ABSTRACT OF THE THESIS

Mechanism of Neurotransmitter-Receptor Matching
in Embryonic Skeletal Muscle *in vivo*

by

Yunxin Wang

Master of Science in Biology

University of California San Diego, 2018

Professor Nicholas Spitzer, Chair

Neurotransmitter switching is associated with behavioral changes in every case that a behavior change has been sought, including levels of anxiety (Dulcis et al., 2013) and motor coordination (Li et al., 2016) in adult rodents (see Spitzer, 2017 for review). To preserve synaptic function, a newly expressed neurotransmitter requires the expression of matching receptors, but the mechanisms by which this is achieved remain unclear. To investigate neurotransmitter-receptor

matching in vivo, *Xenopus laevis* embryos were implanted with drug-loaded agarose beads at the time of closure of the neural tube. Glutamate, a major excitatory neurotransmitter, and the NMDA receptor, an ionotropic glutamate receptor, were chosen as the neurotransmitter-receptor pair in this study. Immunohistochemical analysis revealed that an NMDA receptor subunit GluN1 increased in expression in the trunk muscle plasma membrane in response to glutamate-loaded beads compared to control beads. The upregulation of GluN1 was reproduced with agonists AMPA and NMDA in combination, and suppressed with AP5 (NMDAR antagonist) and NBQX (AMPAR antagonist) in combination, establishing specificity of this receptor upregulation. We established the role of mitogen-activated protein kinases (MAPKs) p38 and jun-N-kinase (JNK) as downstream effectors of glutamate signaling, as well as the role of transcription factor MEF2C as a p38 target, by pharmacological knock-down with morpholinos. We propose a model in which glutamate acts on low numbers of ionotropic glutamate receptors initially expressed on embryonic *Xenopus* muscle (Borodinsky & Spitzer, 2007), promoting calcium entry that activates MAP kinases p38, JNK and MEF2, leading to upregulation of NMDAR expression.

INTRODUCTION

NMDA Receptor

Glutamate receptors are classified into ionotropic and metabotropic types. N-Methyl-D-aspartic acid (NMDA) receptor and α-amino-3-hydroxy-5-methyl-4-isoxazolepropionic acid (AMPA) receptor are two classes of ionotropic glutamate receptors. Functional NMDA receptors are composed of three types of subunits: GluN1 (NR1), GluN2 (encoded by NR2A–2D) (Hollmann and Heinemann, 1994), and GluN3 (encoded by NR3A/3B) (Andersson et al., 2001). GluN1 is a principal subunit for NMDA receptor channel activity and is present in all functional NMDARs (Moriyoshi et al., 1991), while GluN2 and GluN3 subunits determine the specificity of receptor function (Stern et al., 1992, Chatterton et al., 2002).

Neuromuscular Junction

At the *Xenopus laevis* neuromuscular junction, the motor neuron normally expresses acetylcholine (ACh) and muscle cells express ACh receptors (AChR). However, muscle cells express low levels of many receptors at early stages, and lose all of them except AChR following innervation (Borodinsky & Spitzer, 2007). Changes in electrical activity of these immature motor neurons during a critical period can drive a homeostatic shift to non-cholinergic neurotransmitters and the retention of matching receptors from the initially diverse receptor pool. Reduced activity results in a switch from ACh to combinations of cholinergic and glutamatergic phenotypes, with the retention and upregulation of both ionotropic ACh and glutamate receptors in the postsynaptic cell (Borodinsky & Spitzer, 2007). The mechanism of receptor matching remains elusive.

Glutamate-Receptor Matching *in vitro*

The mechanism of glutamate-receptor matching *in vitro* has been investigated with *Xenopus* neuron and myocyte co-cultures and myocyte-only cultures by Dr. Dena Hammond-Weinberger (manuscript in preparation). Exogenous glutamate alone induced the glutamate sensitivity increase in myocytes cultured in calcium medium in the absence of neurons, mimicking the increase found in neuron-myocyte co-cultures in the absence of extracellular calcium (Borodinsky & Spitzer, 2007). Glutamate-induced glutamate sensitivity in myocyte cultures was blocked by simultaneous application of ionotropic receptor antagonists (2R)-amino-5-phosphonovaleric acid (AP5) and 2,3-dihydroxy-6-nitro-7-sulfamoyl-benzo[f]quinoxaline-2,3-dione (NBQX) in combination, but not by an NMDAR antagonist or AMPAR antagonist alone, suggesting that neurotransmitter glutamate acting through low levels of ionotropic receptors NMDAR and AMPAR is both sufficient and necessary to induce glutamate sensitivity increase in myocyte cultures. Metabotropic glutamate receptors were found to make no contribution to the increase in glutamate sensitivity.

Western blots of extracts from glutamate-exposed myocyte cultures showed an increase in NMDAR and AMPAR subunits GluN1 and GluA1 associated with increased glutamate sensitivity, suggesting that glutamate acts through low levels of ionotropic glutamate receptors to upregulate NMDAR and AMPAR expression in skeletal myocytes.

In the present work, *Xenopus laevis* embryos were subjected to local, sustained glutamate exposure during an early period of development to determine whether glutamate acting through low levels of NMDAR and AMPAR is both sufficient and necessary to induce NMDAR upregulation *in vivo*.

MAP Kinases

Mitogen-activated protein kinases (MAPKs) are a family of serine/threonine protein kinases involved in a wide range of cellular processes. Two MAP kinases, c-Jun N-terminal kinases (JNK1, JNK2, JNK3 (Gupta et al., 1996)) and p38 (p38α, β, γ, and δ) can phosphorylate the DNA binding protein c-Jun (Hibi et al., 1993) and transcription factor MEF2 (Han et al., 1997), respectively. Both JNK and p38 can be activated by glutamate-induced NMDAR activation. Glutamate signals through NMDAR to activate JNK and phosphorylate AP-1 proteins that bind to the AP-1 site on DNA (Schwarzschild et al., 1997). NMDAR activation also leads to calcium-dependent activation of p38 (Kawasaki et al., 1997, Waxman and Lynch, 2005). Neither of these pathways appears dependent on protein kinase A (PKA). MEF2 is a Ca2+-sensitive p38 target that binds the GluN1 promoter and regulates its transcription (Krainc et al., 1998).

Dr. Weinberger's work in vitro discovered that adenylate cyclase (AC), but not PKA, acts as a downstream effector of glutamate signaling, suggesting that glutamate receptor upregulation is AC-dependent and PKA-independent. This led to further exploration of p38 and JNK pathways, which confirmed that glutamate sensitivity induced by exogenous glutamate is both p38β- and JNK1-dependent *in vitro*. Vivo-morpholinos were used in the present work to test the necessity of p38β, JNK1 and MEF2C in glutamate-induced NMDAR regulation in myocytes *in vivo*. Vivo-morpholinos achieve intracellular antisense morpholino delivery via conjugation to arginine-rich delivery peptides (Morcos et al., 2008).

METHODS

Generation of Embryos

Adult *Xenopus laevis* females were injected with human chorionic gonadotropin (Merck) to induce ovulation. Oocytes were fertilized *in vitro*. Embryos were grown in 0.1× Marc's modified Ringer's solution (MMR: NaCl (100 mM), KCl (2 mM), $MgSO_4$(1 mM), HEPES (5 mM), EDTA (0.1 mM), $CaCl_2$(2 mM) in Fisher water, pH 7.8) and larvae were staged according to Nieuwkoop and Faber (1967). For each experiment, a total of four different pairs of females and males were used, each generating an independent batch of at least 50 healthy embryos.

Bead Implantation

Spatial and temporal control of delivery of pharmacological agents was achieved by using agarose beads (100-200 mesh, Bio-Rad). Beads were washed in 2 mM calcium saline (NaCl (116 mM), KCl (0.7 mM), $MgSO_4$ (1.3 mM), $CaCl_2$ (2.3 mM), Tris base (4.6 mM) in Fisher water, pH 7.8) for 3 hr at 22°C, replacing washing solution every 20 min, and loaded for 2 hr at 4°C on a bi-directional rotator with 2 mM calcium saline containing drugs (2 mM Glutamate, 10 μM NMDA and 10 μm AMPA (Cayman Chemical), 0.5 mM AP5 and 0.15 mM NBQX (Tocris)), vivo-morpholinos (10 μM, GeneTools), or 2 mM calcium saline (control). Drug concentrations were 10× the concentration tested in myocyte cultures (Weinberger et al., manuscript in preparation), to compensate for dilution during diffusion (Dulcis and Spitzer, 2008). Beads of 120 μm diameter were selected and implanted adjacent to anterior neural tube between the skin and myotome at stage 21 (1 day after fertilization). Each experimental group contained 4-8 bead-implanted embryos, which were allowed to develop to stage 40 (2.8 days after fertilization) and processed for immunohistochemistry (**Figure 1A)**.

Morpholinos

Vivo-morpholinos are cell-permeable morpholinos. Beads loaded with vivo-morpholinos targeting JNK1/MAPK8 (5' TGCTGTCACGCTTGCTTCGGCTCAT-3' Yamanaka et al., 2002), MEF2C (5'-CCATAGTCCCCGTTTTTCTGTCTTC-3′ Guo et al., 2014), and p38β (5' CGCCCGCTCATCTTGCCCCGACCGG-3' GeneTools, Philomath, OR) were used to temporally and spatially restrict knockdown of translation. GeneTools' standard oligo morpholino (5'-CCTCTTACCTCAGTTACAATTTATA-3') was used as a control for morpholinos.

Labeling of Neurotransmitter Receptors

Larvae were fixed at stage 40 in 4% paraformaldehyde/0.025% glutaraldehyde/PBS (pH 7.4) for 30 min at 22°C and rinsed three times in phosphate buffered saline (PBS), 10 min each. Skin was removed from fixed larvae with forceps to allow immunostaining of the myocyte surface membrane. Skinned larvae were incubated for 30 min at 22°C in 1% goat serum/1% fish gelatin/PBS blocking solution followed by overnight incubation with 1:250 primary antibody targeting the C-terminus of the GluN1 subunit (Millipore MAB 363, 1 mg/mL) at 4°C. After three PBS rinses, larvae were incubated for 2 hr with 1:500 fluorescently tagged secondary antibodies (Alexa 488) at 22°C. Immunostained larvae were rinsed three times in PBS, sunk in 80% glycerol/PBS for 30 min and imaged on bridged glass slides on a Leica SP5 confocal microscope with a 20× water immersion objective and appropriate excitation and emission filters for Alexa 488. 2% laser power and digital 1.5× zoom were used to acquire images 517 μm in width that included two muscle chevrons starting at the first intact chevron immediately posterior to the beaded chevron (**Figure 1A, 1B**). *Z*-stacks (1.13 μm steps) were acquired to generate through-series projections starting at the surface of myofibers and extending down to the surface of

notochord, generating an image stack 30-100 μm thick. Stack thickness was within 10 μm variance for each batch of independent experiments.

Image Analysis

Images originally in green (Alexa 488) were converted to black and white and analyzed with Image J. Maximum projection images were generated and the area of intensity analysis of whole mount immunostained preparations was drawn to include two chevrons of muscle but exclude tissue edges, damage, skin (if any), and pigment. The percent of GluN1-labeled area was determined by measuring the fraction occupied by pixels of intensity at or below an empirically determined constant threshold (**Figure 2**). For each batch of embryos, the threshold was set to label 2-5% of control tissue, following the expression level reported by Borodinsky and Spitzer (2007), to allow aggregation of data from independent batches. The percent of labeled area of each image was then subtracted by the percent of labeled area of a control larva from the same clutch of embryos without GluN1 staining to eliminate secondary antibody background labeling. Imaging and data analysis parameters were kept constant within each independent experiment.

Statistics

Means, standard deviations and p values were calculated using GraphPad Prism 7. Unpaired Student's *t*-tests were used for comparisons between two groups. Values were considered significantly different at *$p<0.05$; **$p<0.01$; ***$p<0.001$, ****$p\leq0.0001$.

RESULTS

Signaling through ionotropic glutamate receptors is sufficient and necessary to induce NMDAR upregulation in the embryonic skeletal muscle membrane *in vivo*

Single agarose beads loaded with saline, glutamate (2 mM) or AMPA (10 μM) and NMDA (10 μM) in combination were implanted at stage 21 and larvae were fixed for immunohistochemical processing at stage 40. Bead-implanted tadpoles tolerated the implantation and appeared healthy and active. Beads were consistently placed and remained located in the anterior trunk myocytes. The region of interest was drawn to include two intact myocyte chevrons adjacent to the bead to quantify effects of drug diffusion from the bead (**Figure 1A**). Quantification of representative images shows that immunostaining labeled 2.7% and 12.4% of the dashed area as GluN1 positive in the control and the glutamate image, respectively (**Figure 1B and Figure 2**). GluN1 expression in tadpoles subjected to glutamate bead implantation was compared with expression in tadpoles subjected to saline bead implantation (control) in all experiments. GluN1 quantification showed that glutamate-stimulated tadpoles (n=99) had significantly higher GluN1 expression than control tadpoles (n=108), demonstrated in Figures 5 and 6. In contrast to cell surface labeling, whole-cell labeling with detergent (0.1% Triton) in the fixative showed nuclear staining and a much higher percentage of labeling, with a 21.6% GluN1 upregulation (n=73, control; n=72, glutamate) compared to 9.7% without detergent (n=108, control; n=99, glutamate) (**Figure 1C**). Intracellular GluN1 was not of interest in this study, and Triton was therefore excluded in immunohistostaining to eliminate nuclear GluN1 staining. Of note, saline bead implantation induced a baseline upregulation of GluN1 by 2.1% compared to non-bead-implanted embryos possibly due to tissue inflammation (**Figure 3**; n=3). Previous evidence suggests that

inflammation can induce NMDAR activation (Ren et al., 1992; Schaible et al., 1991), which could result in more GluN1 being expressed or transported to the cell surface.

Data from each of the four batches of embryos showed a significant increase in GluN1 expression in response to implantation of beads loaded with glutamate (2 mM), and the increase was reproduced by implanting beads containing equimolar AMPA and NMDA (10 μM) (**Figure 4**; n=4 independent experiments), suggesting that both glutamate and glutamate receptor agonists are effective in increasing myocyte glutamate receptor expression *in vivo*. Compared to 2 mM glutamate, AMPA and NMDA were administered at a lower concentration due to their high specificity in activating AMPA and NMDA receptors. Pooled data from n=54 embryos showed significant GluN1 upregulation from chronic glutamate and AMPA/NMDA stimulation (**Figure 5A**). Exogenous glutamate stimulation significantly increased GluN1 expression by 11.2% (****$p<0.0001$), whereas AMPA and NMDA in combination significantly increased GluN1 expression by 9.9% (****$p<0.0001$), comparable to glutamate-induced GluN1 upregulation. Receptor upregulation was blocked when NMDAR and AMPAR antagonists AP5 (0.5 mM) and NBQX (0.15 mM) were included with or without glutamate in the beads (**Figure 5B**; n=4 independent experiments). Neither administration of AP5/NBQX or AP5/NBQX plus glutamate was able to produce significantly different GluN1 expression compared to control. These results suggest that chronic glutamate stimulation alone, acting through low levels of ionotropic receptors, is both sufficient and necessary to induce increased NMDAR expression in the myocyte *in vivo*.

p38 and JNK pathways are required for glutamate-induced NMDAR upregulation

Studies by previous investigators suggested a signaling transduction cascade involving MAP kinases (**Figure 7**, Weinberger et al., manuscript in preparation). Morpholinos are an

effective way to knockdown gene expression in *Xenopus* as well as in some other species (Ferguson et al., 2014). The specificity of morpholinos to JNK1 (Yamanaka et al., 2002), p38β (Ohnishi et al., 2010) and MEF2C (Guo et al., 2014) has previously been validated in *Xenopus*. Gene knockdown of JNK1 using vivo-morpholinos delivered with agarose beads blocked glutamate-mediated NMDAR upregulation *in vivo* (n=22), confirming the role of JNK1 as a critical downstream effector of glutamate signaling (**Figure 6A**; n=4 independent experiments). Glutamate-induced NMDAR upregulation was also blocked by p38β knockdown (n=19), confirming that p38β is required for the upregulation of glutamate receptors (**Figure 6B**; n=4 independent experiments). As a p38 target, the effect of knocking down MEF2C was tested to establish the requirement for MEF2 in glutamate-mediated upregulation of NMDAR. Implantation of beads loaded with MEF2C and glutamate (n=19) abrogated the upregulation of GluN1 achieved by glutamate alone (**Figure 6C**; n=4 independent experiments). Student's *t*-test was used to compare experimental groups pairwise and draw the conclusions below. In all three morpholino experiments, glutamate induced a significant GluN1 increase compared with control, control morpholino, and experimental morpholinos with or without glutamate (****$p<0.0001$). The differences in GluN1 expression between saline and control morpholino were not significant ($p>0.1$), confirming the absence of a non-antisense effect of morpholino exposure (**Figure 6A, B and C**). JNK1, p38β and MEF2C morpholinos alone had non-significant effects on GluN1 expression when compared with control ($p>0.17$). However, glutamate was not able to significantly change GluN1 expression in the presence of any one of these three morpholinos, indicating the necessity of JNK1, p38β and MEF2C in glutamate-mediated NMDAR upregulation. All experiments were done with four independent clutches of embryos generated from four pairs of parents; each clutch showed significant effects with the same pattern observed in Figure 6.

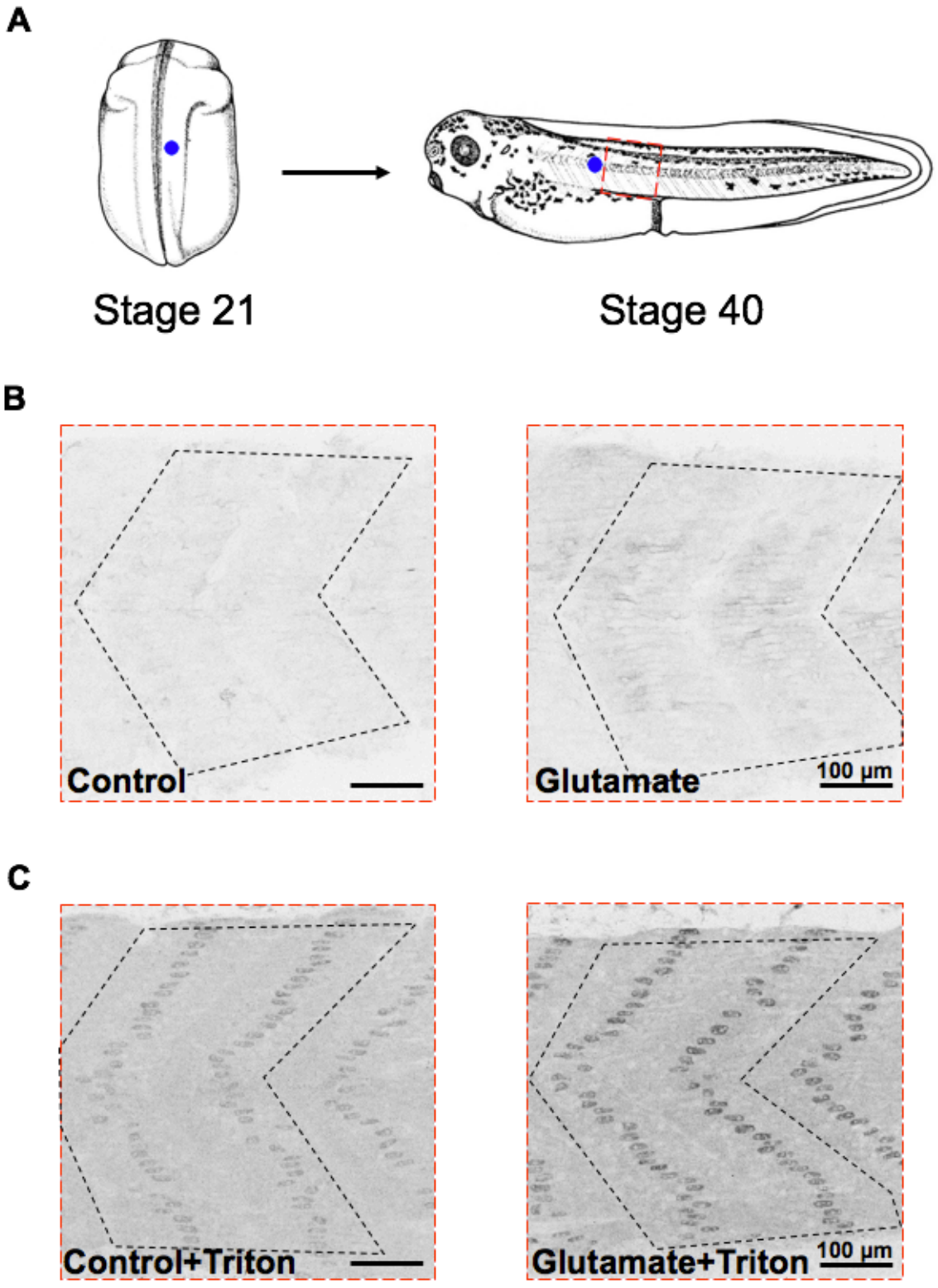

Figure 1. Sustained delivery of glutamate increases myocyte plasma membrane expression of GluN1. A. Schematic of experimental design. Stage 21 embryos were subjected to agarose bead

(Figure 1. Continued) (blue) implantation and allowed to grow to stage 40 (2.8 days after fertilization). Confocal images of two muscle chevrons were taken starting at the first intact chevron posterior to the bead (red square). **B.** Representative images show that glutamate delivered by the agarose bead stimulated an increase in cell surface membrane GluN1 immunoreactivity at 2.8 days post fertilization in trunk myocytes. Two muscle chevrons (black dashed lines) are included in GluN1 quantification. 2.7% of the outlined area is labeled by GluN1 immunohistochemistry in a control larva and 12.4% area is labeled in a glutamate-stimulated larva. **C.** Representative images showing whole-cell immunohistochemistry following Triton exposure in control and glutamate-stimulated embryos reveal glutamate-dependent nuclear GluN1 staining in myocytes *in vivo*. Whole-cell staining labels 14.2% and 35.8% of two muscle chevrons (black dashed lines) as GluN1 positive pixels. A greater glutamate-induced increase in surface membrane GluN1 immunoreactivity is observed in the presence of Triton. Scale bar, 100 μm.

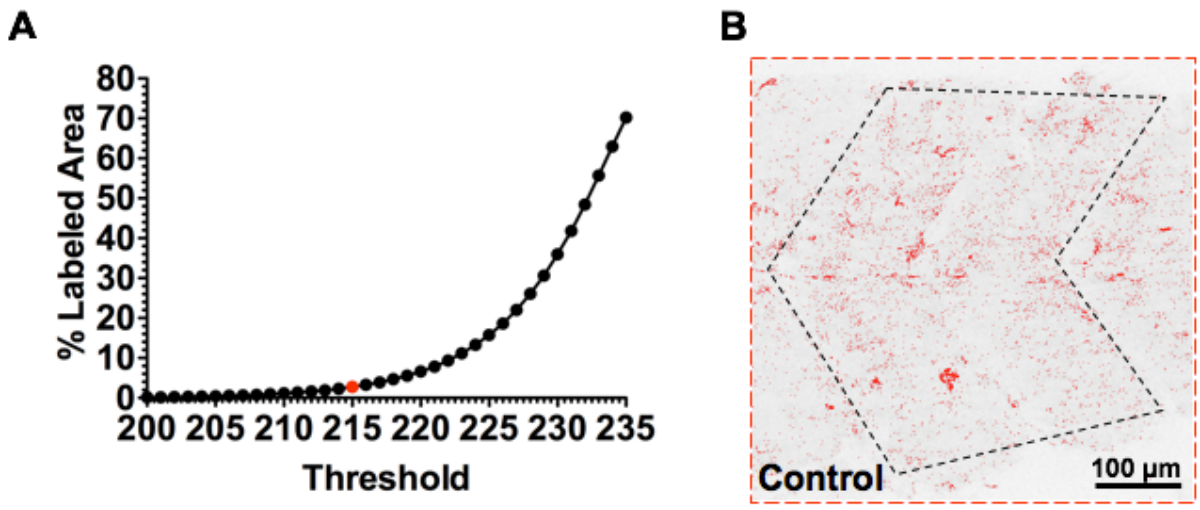

Figure 2. ImageJ calculates image pixel intensity of a representative saline bead-implanted myocyte. A. The percentage of pixels at or below an empirically determined threshold increases as threshold is increased. **B.** Percentage of area labeled as GluN1-immunoreactive at or below a threshold of 215 (red). Scale bar, 100 µm.

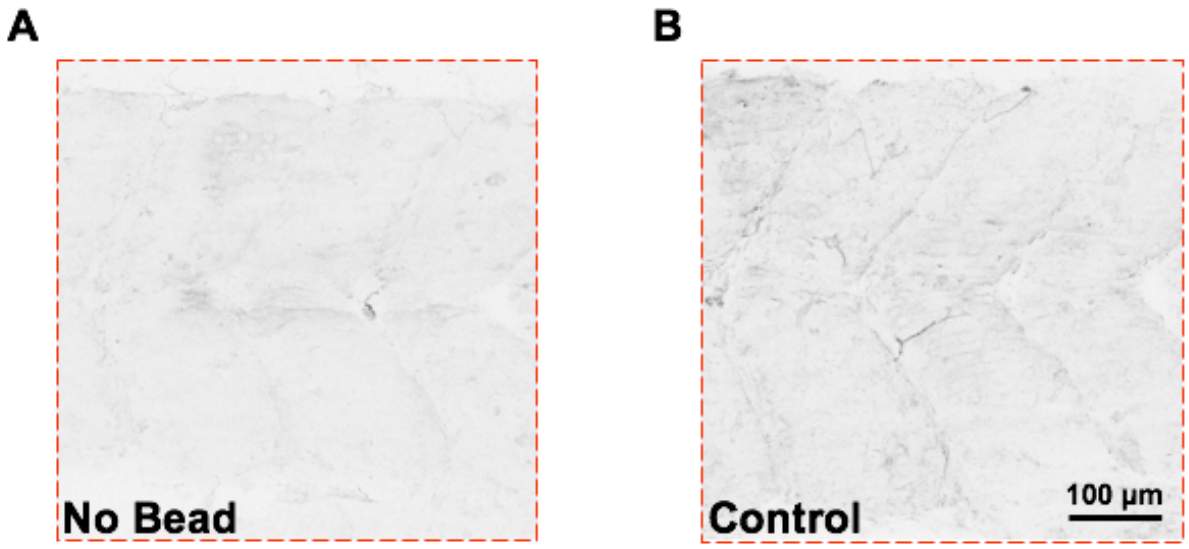

Figure 3. Bead implantation induces modest background GluN1 upregulation in myocytes *in vivo*. Representative non-bead-implanted (**A**) and saline bead-implanted (**B**) images show 0.4% and 2.5% of GluN1 immunoreactivity, respectively. Scale bar, 100 µm.

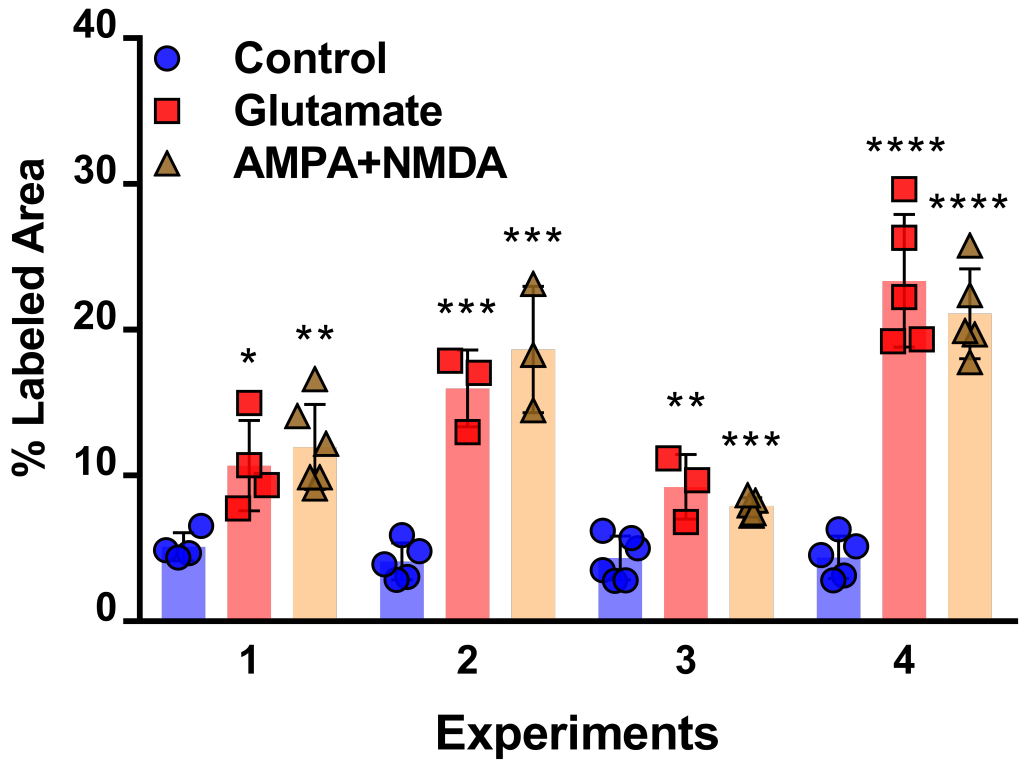

Figure 4. Bead delivery of glutamate and glutamate agonists induce GluN1 upregulation on myocytes *in vivo*. The percentage of GluN1+ pixels from independent batches shows significant GluN1 upregulation with glutamate (2 mM) and with equimolar AMPA plus NMDA (10 μM) stimulation for each experiment. Graph shows mean ± SD. N=4 independent experiments. Unpaired Student's *t*-test between asterisked groups and respective controls, *p<0.05; **p<0.01; ***p<0.001, ****p≤0.0001.

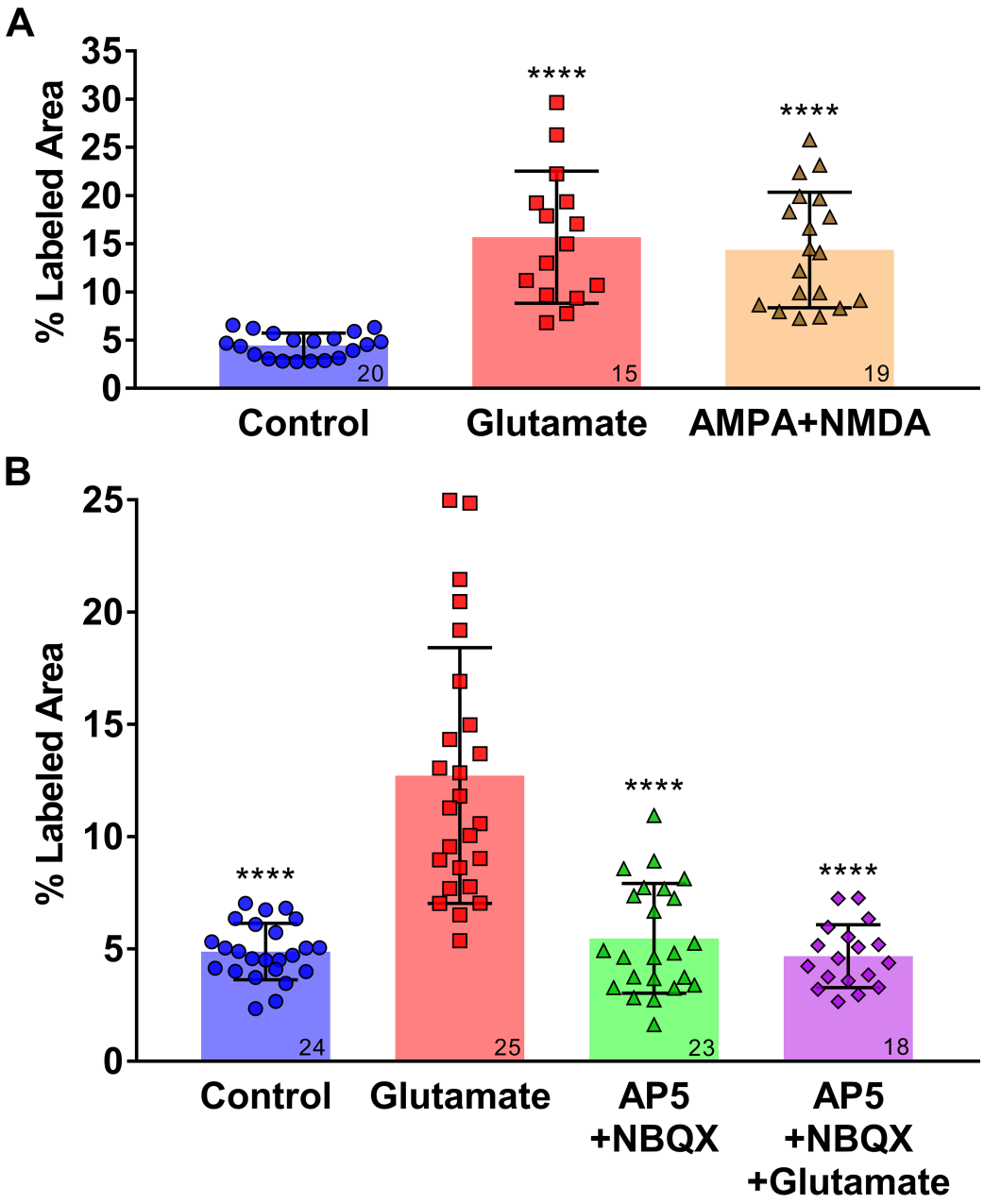

Figure 5. Glutamate signaling to ionotropic receptors is necessary and sufficient to induce glutamate sensitivity of trunk myocytes *in vivo*. A. Glutamate induces GluN1 upregulation 3.5-fold; agonists AMPA and NMDA induce GluN1 upregulation 3.2-fold. In both cases, the increase in GluN1 expression is significant (****$p<0.0001$) compared to control. **B.** Glutamate-induced GluN1 upregulation is completely abrogated by simultaneous application of antagonists AP5 and NBQX. GluN1 expression with antagonist administration is significantly lower than glutamate administration (****$p<0.0001$) but not different from control ($p=0.30$). GluN1 expression with antagonist plus glutamate administration is also significantly lower than glutamate alone (****$p<0.0001$) but not different from control ($p=0.63$). Graphs show mean ± SD. N=4 independent experiments for each graph. On each bar, the lower right number insert shows the

(Figure 5. Continued) number of embryos examined. Unpaired Student's *t*-test, *p<0.05; **p<0.01; ***p<0.001, ****p≤0.0001.

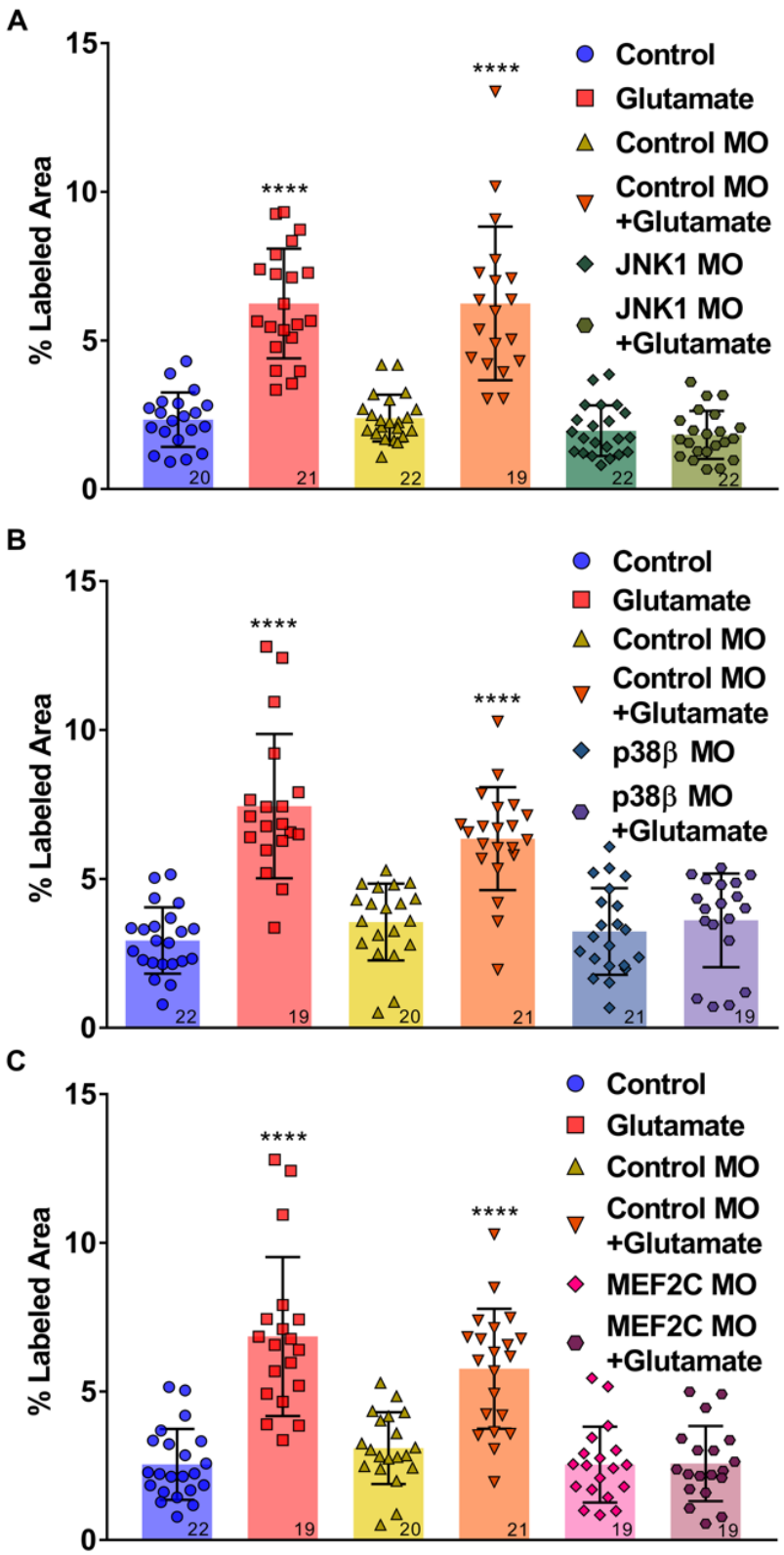

Figure 6. Glutamate-mediated GluN1 upregulation is abrogated by JNK1, p38β, or MEF2C suppression *in vivo*. A. GluN1 upregulation is abrogated by JNK1 knockdown with morpholino.

(Figure 6. Continued) **B.** Morpholino-mediated p38 knockdown eliminates the effect of glutamate on increased GluN1 expression. **C.** GluN1 upregulation is abolished by MEF2C knockdown. In all three experiments, the control morpholino plus or minus glutamate recapitulates the no-morpholino control group plus or minus glutamate. JNK1, p38β and MEF2C morpholinos alone have no significant effect in GluN1 expression compared to control. Within the groups of saline, control morpholino, and experimental morpholinos with or without glutamate, no significant difference is present between any group pairs. Glutamate is not significantly different from control morpholino plus glutamate ($p>0.1$) in all three experiments. Graphs show mean ± SD. N=4 independent experiments for each graph. On each bar the lower right number insert shows the number of embryos examined. Unpaired Student's *t*-test, *$p<0.05$; **$p<0.01$; ***$p<0.001$, ****$p\leq0.0001$.

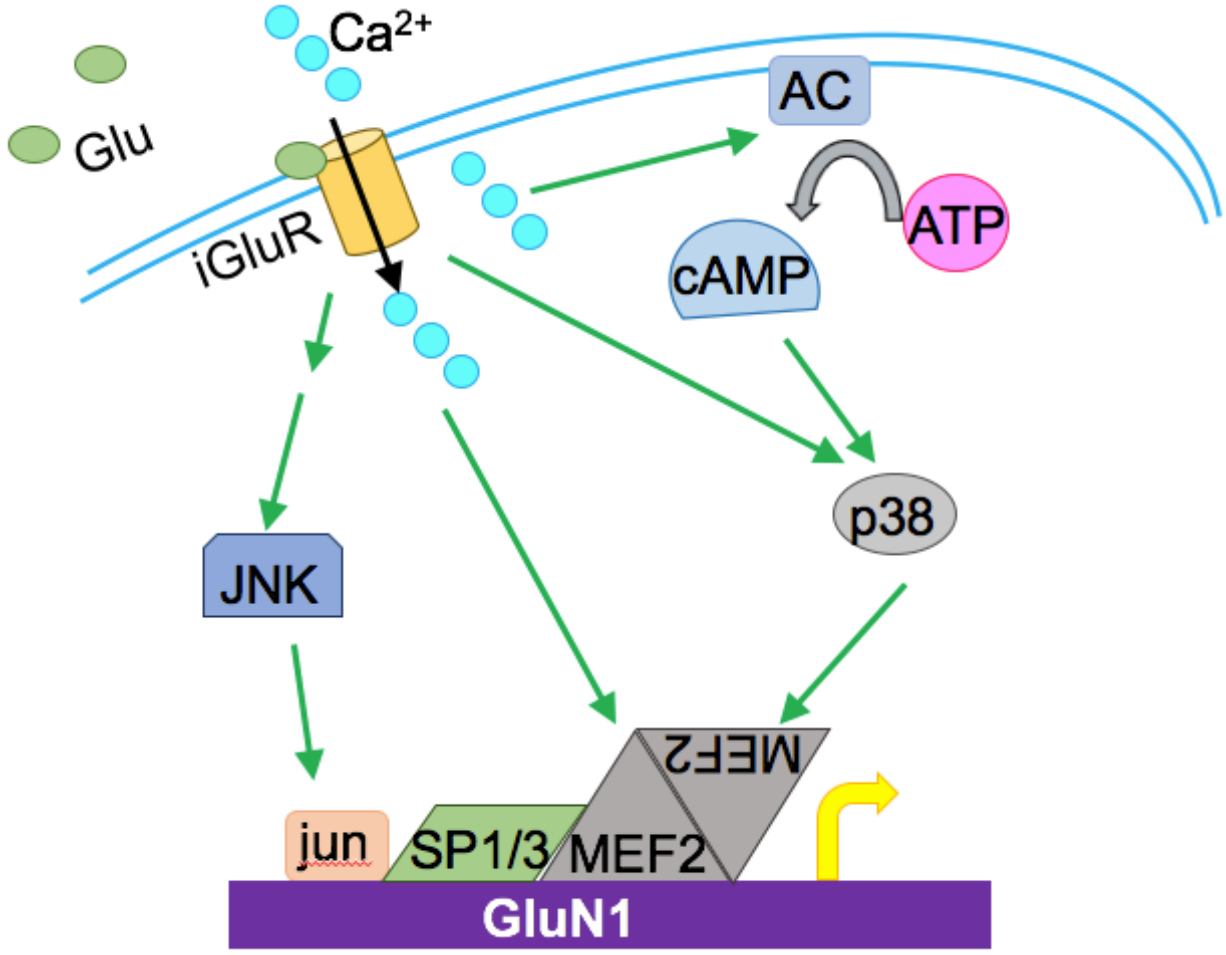

Figure 7. Proposed model showing the signaling cascade by which glutamate acts on ionotropic receptors to induce NMDAR upregulation that is JNK1-, p38β- and MEF2C- dependent in trunk myocytes *in vivo*.

DISCUSSION

Neurotransmitter switching is defined as the loss of one neurotransmitter and the gain of another. It has been identified in many systems to be associated with behavioral change, but the mechanisms by which neurotransmitter receptors match a newly expressed transmitter to allow behavioral change remain unknown. Unpublished data in the Spitzer lab has established a pathway leading to NMDA receptor upregulation in *Xenopus* trunk myocytes induced by exogenous glutamate *in vitro*, involving MAP kinase pathways JNK and p38. In the present study, similar findings were established *in vivo* with *Xenopus* trunk myocytes. Glutamate acting through low levels of ionotropic receptors was found to be both sufficient and necessary to induce NMDAR upregulation. This upregulation was suppressed by JNK1, p38β and MEF2C knockdowns with morpholinos.

Glutamate acts through ionotropic receptors to induce NMDAR upregulation

Sustained glutamate release on *Xenopus* trunk myocytes by agarose bead implantation starting at the time of neural tube closure induced cell-surface NMDA receptor upregulation by 2-3 fold, quantified with GluN1 immunohistochemistry and confocal image pixel intensity analysis. NMDA and AMPA in combination were able to elicit NMDAR upregulation similar to that achieved by glutamate, establishing that glutamate acting through low levels of NMDAR and AMPAR is sufficient to enable NMDAR upregulation. Glutamate-mediated GluN1 upregulation was blocked by a combination of the NMDAR antagonist, AP5, and the AMPAR antagonist, NBQX, indicating that NMDAR and AMPAR activation are necessary for glutamate-induced NMDAR upregulation. Changes in GluN1 expression were all compared with tadpoles subjected to saline bead implantation (control), which demonstrated a modest baseline GluN1 increase compared to control bead implantation, possibly due to inflammation.

In addition to the effect of chronic stimulation, NMDAR upregulation also occurs in response to acute stimuli triggering long-term potentiation, contributing to synapse plasticity and learning. NMDA receptor activation allows calcium influx, which induces immediate activation of a variety of proteins associated with the receptors inside the cell. Among these are Ca^{2+} calmodulin-dependent protein kinases responsible for long-term potentiation, a process involved in long lasting neuronal memory formation and learning (Malinow et al., 1989). Future research may explore potential therapeutic benefits of implanting glutamate release devices to increase synaptic strength, long-term potentiation and learning.

Glutamate-induced NMDAR upregulation is JNK1-, p38β- and MEF2C-dependent

MAPKs regulate cellular responses to a variety of extracellular signals (e.g. osmotic stress, heat shock, cytokines, and mitogens) and affect cell division, differentiation, and apoptosis. In the present study, MAPKs were found to be involved in glutamate-mediated NMDAR upregulation *in vivo*. Glutamate-induced cell-surface GluN1 upregulation was abrogated by JNK1, p38β, or MEF2C knockdowns. These results suggest that glutamate acts on low levels of ionotropic receptors to activate JNK1, p38β and MEF2 (**Figure 7**). JNK phosphorylates DNA-binding AP-1 proteins including transcription factor jun (Hibi et al., 1993), which binds to an AP-1 site in the distal promoter of the GluN1 gene (Bai et al., 1993) to regulate its transcription rate. Activated p38 phosphorylates MEF2 (Han et al., 1997), which has its recognition sequence in the GluN1 promoter, to positively regulate GluN1 transcription (Krainc et al., 1998). This evidence suggests that JNK1, p38, and MEF2 are necessary for upregulation of GluN1 expression.

Conclusion

Neurotransmitter switching is a novel form of synaptic plasticity that is associated with behavioral changes in every case that a behavior change has been sought (Grant et al., 1995; Dulcis & Spitzer, 2008; Demarque & Spitzer, 2010; Kanazawa et al., 2010; Dulcis et al., 2013; Olivas et al., 2016; Dulcis et al., 2017; see Spitzer, 2017 for review). These results indicate the possibility of manipulating behaviors clinically by inducing or blocking neurotransmitter switching in higher mammals. Transmitter-receptor matching is necessary for transmitter-switched synapses to remain functional. In the future this process could be targeted by drugs to block neurotransmitter switching. To elucidate the mechanisms of transmitter-receptor matching, *Xenopus laevis* was chosen to study glutamate-induced NMDA receptor upregulation, due to the availability of large numbers of embryos and rapid growth rate. The present work is one of the first steps in studying the mechanism of neurotransmitter-receptor matching *in vivo*. We established that glutamate acting through low levels of ionotropic receptors is sufficient and necessary to induce NMDA receptor upregulation in *Xenopus* trunk myocytes, and that this process is JNK1-, p38β- and MEF2- dependent. It would be useful to focus future experiments on studies of the role of MEF2 *in vitro* and on the mechanism of AMPAR upregulation *in vivo*.

REFERENCES

1. Dulcis D, Jamshidi P, Leutgeb S, Spitzer NC. 2013. Neurotransmitter switching in the adult brain regulates behavior. *Science* 26 APR 2013: 449-453

2. Li H, Jackson KB, Spitzer NC. 2016. Exercise-induced neurotransmitter switching in the adult mouse mid-brain. *2016 Neurosci. Meet. Plan., San Diego*, Program No. 36.01. San Diego, CA: Soc. Neurosci.

3. Spitzer NC. 2017. Neurotransmitter switching in the developing and adult brain. *Annual Review of Neuroscience* 2017, 40:1, 1-19

4. Borodinsky LN, Spitzer NC. 2007. Activity-dependent neurotransmitter-receptor matching at the neuromuscular junction. *Proceedings of the National Academy of Sciences* Jan 2007, 104(1):335-340

5. Hollmann M, Heinemann S. 1994. Cloned glutamate receptors. *Annual Review of Neuroscience* 1994, 17:31-108

6. Andersson O, Stenqvist A, Attersand A, Euler Gv. 2001. Nucleotide sequence, genomic organization, and chromosomal localization of genes encoding the human NMDA receptor subunits NR3A and NR3B. *Genomics* 78(3):178-84

7. Moriyoshi K, Masu M, Ishii T, Shigemoto R, Mizuno N, Nakanishi S. 1991. Molecular cloning and characterization of the rat NMDA receptor. *Nature* 354:31–37

8. Stern P, Béhé P, Schoepfer R, Colquhoun D. 1992. Single-channel conductances of NMDA receptors expressed from cloned cDNAs: comparison with native receptors. *Proceedings of the Royal Society B* 1992, 250, 271-277

9. Chatterton JE, Awobuluyi M, Premkumar LS, Takahashi H, Talantova M, Shin Y, Cui J, Tu S, Sevarino KA, Nakanishi N, Tong G, Lipton SA, Zhang D. 2002. Excitatory glycine receptors containing the NR3 family of NMDA receptor subunits. *Nature* 415:793-798

10. Gupta S, Barrett T, Whitmarsh AJ, Cavanagh J, Sluss HK, Dérijard B, Davis RJ. 1996. Selective interaction of JNK protein kinase isoforms with transcription factors. *The EMBO Journal* 15(11):2760-70

11. Hibi M, Lin A, Smeal T, Minden A, Karin M. 1993. Identification of an oncoprotein- and UV-responsive protein kinase that binds and potentiates the c-Jun activation domain. *Genes & Development 1993* 7: 2135-2148

12. Han J, Jiang Y, Li Z, Kravchenko VV, Ulevitch RJ. 1997. Activation of the transcription factor MEF2C by the MAP kinase p38 in inflammation. *Nature* 386:296-299

13. Schwarzschild MA, Cole RL, Hyman SE. 1997. Glutamate, but not dopamine, stimulates stress-activated protein kinase and AP-1-mediated transcription in striatal neurons. *Journal of Neuroscience* 1997 May 15;17(10):3455-66.

14. Kawasaki H, Morooka T, Shimohama S, Kimura J, Hirano T, Gotoh Y, Nishida E. 1997. Activation and involvement of p38 mitogen-activated protein kinase in glutamate-induced apoptosis in rat cerebellar granule cells. *Journal of Biological Chemistry* Jul 25;272(30):18518–21

15. Waxman EA, Lynch DR. 2005. N-methyl-D-aspartate receptor subtype mediated bidirectional control of p38 mitogen-activated protein kinase. *Journal of Biological Chemistry* Aug 12;280(32):29322–33

16. Krainc D, Bai G, Okamoto S, Carles M, Kusiak JW, Brent RN, Lipton SA. 1998. Synergistic activation of the N-methyl-D-aspartate receptor subunit 1 promoter by myocyte enhancer factor 2C and Sp1. *Journal of Biological Chemistry* Oct 2;273(40):26218-24

17. Morcos PA, Li Y, Jiang S. 2008. Vivo-Morpholinos: a non-peptide transporter delivers Morpholinos into a wide array of mouse tissues. *BioTechniques* 01 Dec 2008, 45(6):613-4, 616, 618 passim

18. Nieuwkoop PD, Faber J. 1967. Normal Table of Xenopus laevis (Daudin). North-Holland Publishing Co., Amsterdam.

19. Dulcis D, Spitzer NC. 2008. Illumination controls differentiation of dopamine neurons regulating behaviour. *Nature* Nov 13;456(7219):195-201

20. Yamanaka H, Moriguchi T, Masuyama N, Kusakabe M, Hanafusa H, Takada R, Takada S, Nishida E. 2002. JNK functions in the non-canonical Wnt pathway to regulate convergent extension movements in vertebrates. *EMBO Reports* Jan 15; 3(1): 69–75

21. Guo Y, Kühl SJ, Pfister AS, Cizelsky W, Denk S, Beer-Molz L, Kühl M. 2014. Comparative Analysis Reveals Distinct and Overlapping Functions of Mef2c and Mef2d during Cardiogenesis in Xenopus laevis. *PLoS ONE* 9(1): e87294

22. Ren K, Hylden JLK, Williams GM, Ruda MA, Dubner R. 1992. The effects of a non-competitive NMDA receptor antagonist, MK-801, on behavioral hyperalgesia and dorsal horn neuronal activity in rats with unilateral inflammation. *Pain* 50(3):331-44

23. Schaible HG, Grubb BD, Neugebauer V, Oppmann M. 1991. The effects of NMDA antagonists on neuronal activity in cat spinal cord evoked by acute inflammation in the knee joint. *European Journal of Neuroscience* Oct 1991, 3(10):981-91

24. Ferguson DP, Dangott LJ, Lightfoot JT. 2014. Lessons learned from vivo-morpholinos: how to avoid vivo-morpholino toxicity. *BioTechniques* 2014; 56(5):251-56

25. Ohnishi E, Goto T, Sato A, Kim MS, Iemura S, Ishitani T, Natsume T, Ohnishi J, Shibuya H. 2010. Nemo-like kinase, an essential effector of anterior formation, functions downstream of p38 mitogen-activated protein kinase. *Molecular and Cellular Biology* 2010 Feb;30(3):675-83

26. Malinow R, Schulman H, Tsien RW. 1989. Inhibition of postsynaptic PKC or CaMKII blocks induction but not expression of LTP. *Science* 25 Aug, 245(4920):862-66

27. Bai G, Kusiak JW. 1993. Cloning and analysis of the 5' flanking sequence of the rat N-methyl-D-aspartate receptor 1 (NMDAR1) gene. *Biochimica et Biophysica Acta* 1993 Oct 10;1152(1):197-200

28. Grant MP, Francis NJ, Landis SC. 1995. The role of acetylcholine in regulating secretory responsiveness in rat sweat glands. *Mol. Cell. Neurosci* 6:32–42

29. Demarque M, Spitzer NC. 2010. Activity-dependent expression of Lmx1b regulates specification of serotonergic neurons modulating swimming behavior. *Neuron* Jul 29;67(2):321-34

30. Kanazawa H, Ieda M, Kimura K, Arai T, Kawaguchi-Manabe H, Matsuhashi T, Endo J, Sano M, Kawakami T, Kimura T, Monkawa T, Hayashi M, Iwanami A, Okano H, Okada Y, Ishibashi-Ueda H, Ogawa S, Fukuda K. 2010. Heart failure causes cholinergic transdifferentiation of cardiac sympathetic nerves via gp130-signaling cytokines in rodents. *Journal of Clininal Investigation* 120:408–21

31. Olivas A, Gardner RT, Wang L, Ripplinger CM, Woodward WR, Habecker BA. 2016. Myocardial infarction causes transient cholinergic transdifferentiation of cardiac sympathetic nerves via gp130. *Journal of Neuroscience* 36:479–88

32. Dulcis D, Lippi G, Stark CJ, Do LH, Berg DK, Spitzer NC. 2017. Neurotransmitter switching regulated by miRNAs controls changes in social preference. *Neuron* Sep 13;95(6):1319-33.e5